

A NEW METHOD FOR IN-FLIGHT DEGRADATION CORRECTION OF GOME-2 EARTH REFLECTANCE MEASUREMENTS, WITH APPLICATION TO THE ABSORBING AEROSOL INDEX

Lieuwe G. Tilstra, Olaf N.E. Tuinder, and Piet Stammes

Royal Netherlands Meteorological Institute (KNMI), Wilhelminalaan 10, De Bilt, The Netherlands

Abstract

In this paper we study instrument degradation affecting the Earth reflectance measurements by the spectrometer GOME-2 onboard MetOp-A using a recently introduced new method. The actual factor describing reflectance degradation is quantified and analysed for a selection of wavelength bands and as a function of scan mirror position. Using the derived set of correction parameters, the GOME-2 reflectance measurements are corrected for instrument degradation and verified using the Absorbing Aerosol Index (AAI) product. Before correction, time series of GOME-2 AAI showed strong signs of instrument degradation. After applying the correction, no remnants of effects of instrument degradation can be found, proving that the in-flight degradation correction method works.

METHOD FOR IN-FLIGHT DEGRADATION CORRECTION

The method for in-flight degradation correction that we use in this paper has been introduced earlier in Tilstra et al. (2012). Nevertheless, a short description of this method will now follow. The method is based on studying time series of the daily global mean reflectance. The daily global mean reflectance, in this paper denoted by R^* , is defined as the mean of all measured Earth reflectances for a certain scan mirror position on a certain day between 60°N and 60°S and with solar zenith angles below 85°. The time series of the global mean reflectances show seasonal variations as well as a trend due to instrument degradation. To analyse the time series, we assume that the global mean reflectance may be well described empirically by a function made up of a polynomial term, representing the reflectance change due to instrument degradation, multiplied by a term periodic in time that represents the normal seasonal variation of the global mean reflectance. In other words,

$$R_{\lambda,s}^* = P_{\lambda,s}^{(p)} \cdot [1 + F_{\lambda,s}^{(q)}], \quad (1)$$

where the term P represents the polynomial part of degree p , defined by

$$P_{\lambda,s}^{(p)}(t) = \sum_{m=0}^p u_{\lambda,s}^{(m)} \cdot t^m, \quad (2)$$

while the seasonal variation F is described by a finite Fourier series of order q , according to

$$F_{\lambda,s}^{(q)}(t) = \sum_{n=1}^q [v_{\lambda,s}^{(n)} \cdot \cos(2\pi nt) + w_{\lambda,s}^{(n)} \cdot \sin(2\pi nt)]. \quad (3)$$

In these equations, the parameter t is the time expressed in years since the beginning of the time series (which is 4 January 2007 in the case of GOME-2 on MetOp-A). The parameter λ refers to the wavelength being studied and the integer s relates to the scan mirror position. For GOME-2, this integer runs from 1 to 32 for the nominal integration time (IT) of 187.5 ms when the instrument scans from east to west and back. Backscan measurements are not considered in this paper. Therefore, s runs from 1 to 24. The polynomial part P is the most important as it represents the relative change in

the GOME-2 measured Earth reflectance over the years, per scan mirror position, due to instrument degradation. Normalisation of P immediately leads to the reflectance degradation factor:

$$d_{\lambda,s}(t) = P_{\lambda,s}^{(p)}(t) / P_{\lambda,s}^{(p)}(0) \quad (4)$$

The correction for instrument degradation can easily be calculated using

$$c_{\lambda,s}(t) \equiv 1/d_{\lambda,s}(t) = P_{\lambda,s}^{(p)}(0) / P_{\lambda,s}^{(p)}(t). \quad (5)$$

The measured Earth reflectances have to be multiplied with these correction factors. For this paper, we selected 9 wavelength bands in the continuum parts of the spectrum, each band being 1 nm wide and centred at wavelengths of 310, 325, 340, 380, 450, 520, 610, 670 and 750 nm. See Figure 1.

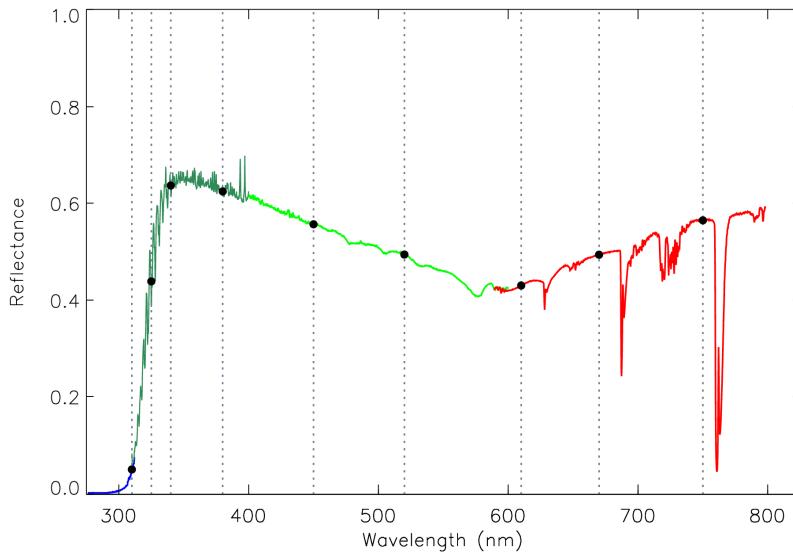


Figure 1: Reflectance spectrum measured by GOME-2 on 3 January 2011. Channels 1 to 4 were given the colours blue, sea green, green, and red, respectively, and channel data in overlap regions were trimmed in order to get a continuous spectrum. The vertical lines combined with the black circles visualise the location of the 9 selected wavelength bands.

ANALYSING GOME-2 INSTRUMENT DEGRADATION

In Figure 2 we present time series of the daily global mean reflectance, measured by GOME-2 at 325 and 380 nm, respectively, for each of the scan mirror positions that make up the orbit swath. The time series cover the period between 4 January 2007 and 24 July 2012, spanning more than 5 years. In order to be able to distinguish between the different reflectance time series, each time series was shifted vertically by +0.05 with respect to the previous one, resulting in an offset of $(s-1) \cdot 0.05$, where s relates to the scan mirror position. The number $s = 1$ refers to the first and easternmost measurement of the forward scan, and the number $s = 24$ to the last and westernmost measurement in the forward scan. Backscan measurements, for which s would run from 25 to 32, were not considered.

The black curves are fits to the data, based on the combination of a Fourier series and a polynomial base as described in the previous section. We took $p = 3$ and $q = 6$. The agreement of the fits with the measured time series is very good. Notice that the noise of the 380-nm time series is clearly higher than that of the 325-nm time series. This is a direct result of the fact that the natural variation in scene reflectance gets larger as the wavelength increases because the surface contribution increases with wavelength. The increased noise has no noticeable impact on the quality of the fit and the retrieved fit parameters. The blue monotonous curves shown in Figure 2 represent the polynomial part P and therefore directly describe the observed reflectance change due to instrument degradation.

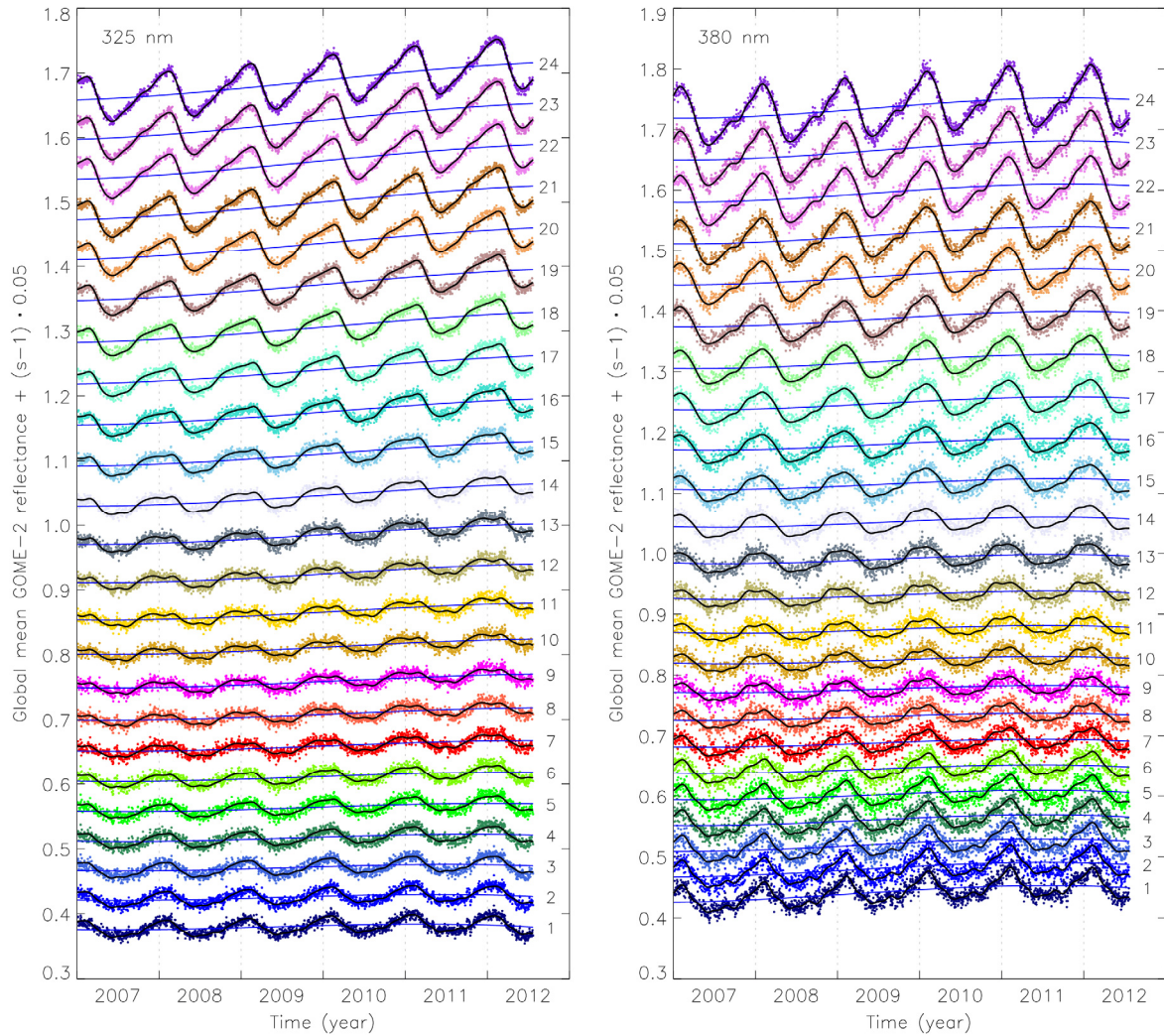


Figure 2: Global mean reflectance measured by GOME-2 at 325 nm (left) and 380 nm (right) as a function of time, for each of the 24 scan mirror positions in the forward scan. To separate the time series graphically, an offset of $(s-1) \cdot 0.05$ was added to each, where s is the scan mirror position as indicated. The solid black curves are fit results and are described in the main text. The blue monotonous curves illustrate the effect of instrument degradation over the years.

The increase in the GOME-2 reflectance is a direct result of the fact that the decrease in the measured GOME-2 Earth radiance is lower than the decrease in the measured GOME-2 solar irradiance. That is, the measured solar irradiance is degrading at a faster rate than the measured Earth radiance.

Figure 3 presents the reflectance degradation factor retrieved at 340 nm, as a function of time for all scan mirror positions in the GOME-2 forward scan. As defined before in equation (4), the reflectance degradation factor is the polynomial part P normalised to unity at the start of the time series (which is 4 January 2007). Clearly, there is a strong and growing scan-angle dependence that results in an east-west bias of up to 7% halfway the year 2012. The impact of instrument degradation on the measured Earth reflectance (at 340 nm) has reached the 10% level. To also study the wavelength dependence of the instrument degradation, we focus on a near-nadir GOME-2 scan mirror position ($s = 13$) and plot the reflectance degradation factor as a function of time for several wavelength bands in Figure 4. Note that the time series of the wavelength bands of 450 nm and higher only go up to the end of 2010. This is due to the fact that our data processing activities were split into several distinct fragments. In general, one can say that the effect of instrument degradation on the measured GOME-2 Earth reflectance is (1) an increase with time and (2) a decrease in magnitude with increasing wavelength.

However, for the wavelength bands at 610, 670, and 750 nm, for which we would not expect to find any significant signs of instrument degradation, the retrieved reflectance degradation factor does show

a clear time dependence with first a decrease and then an increase. This is pointing to the existence of more than one component that is responsible for the radiometric change. Such a component may, for instance, be related to the effects of instrument degradation on the GOME-2 polarisation measurements and the resulting correction. In any case, it is important to stress that the proposed method to correct for instrument degradation does not make any assumptions beforehand about the exact nature and behaviour of the instrument degradation. It only assumes that the Earth is stable in the period considered. In the next section we will include the in-flight degradation correction into the retrieval of the GOME-2 Absorbing Aerosol Index (AAI) product. The main goals here are to present a possible application and to verify the correctness of the applied degradation correction parameters.

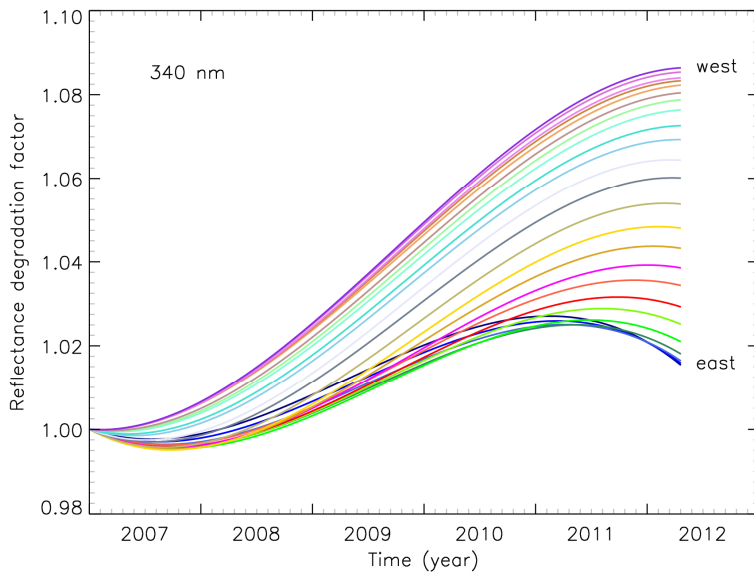


Figure 3: Retrieved reflectance degradation factor for the wavelength band at 340 nm as a function of time, for each of the 24 scan mirror positions. Fit parameters are $p = 3$ and $q = 6$. The meaning of the colours is the same as in Figure 2.

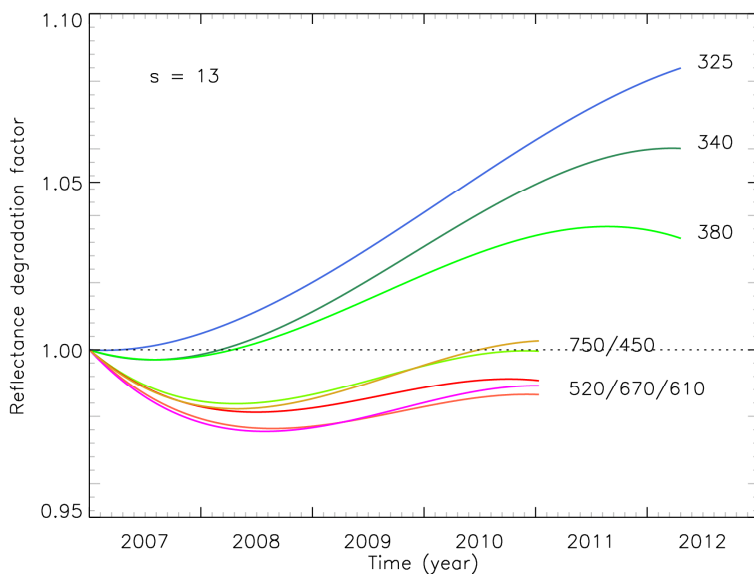


Figure 4: Retrieved degradation factor for the westernmost scan mirror position as a function of time, for several UV and visible wavelength bands. The time series for 450 nm and up stop at the end of 2010. Instrument degradation is strongest in the UV and is more or less decreasing in magnitude with increasing wavelength.

APPLICATION TO THE ABSORBING AEROSOL INDEX

GOME-2 Absorbing Aerosol Index

The Absorbing Aerosol Index (AAI) is an index based on a comparison of measured UV reflectances with simulated Rayleigh reflectances. These simulated reflectances are calculated for cloud-free and aerosol-free atmospheres in which only Rayleigh scattering, absorption by molecules, Lambertian surface reflection as well as surface absorption can take place. The AAI itself is derived from another quantity, called the residue, which is defined as

$$r = -100 \cdot \log_{10} \left(\frac{R_{\lambda}^{\text{obs}}}{R_{\lambda}^{\text{Ray}}} \right). \quad (6)$$

In this equation, R^{obs} refers to reflectances measured by, in this case, GOME-2, while R^{Ray} refers to modelled Rayleigh reflectances. The symbol λ refers to the first, shortest wavelength of the AAI wavelength pair, which is 340 nm. The surface albedo A_s used in the simulations for this wavelength is assumed to be the same as the surface albedo at the second wavelength $\lambda_0 = 380$ nm. The surface albedo at 380 nm on its turn is found from requiring that the simulated Rayleigh reflectance equals the measured reflectance at this wavelength. That is, we have the following two constraints:

$$R_{\lambda_0}^{\text{obs}} = R_{\lambda_0}^{\text{Ray}}(A_s) \quad \text{and} \quad A_s(\lambda) = A_s(\lambda_0) \quad (7)$$

The two equations above basically define the algorithm that is used to calculate the residue. When a positive residue is found, absorbing aerosols were detected. Negative or zero residues on the other hand suggest an absence of absorbing aerosols. Therefore, the AAI is defined as equal to the residue where the residue is positive, and it is simply not defined for negative values of the residue. Note that negative residues in cloud-free conditions can sometimes be interpreted as indicators of the presence of scattering aerosols. See, for instance, Penning de Vries et al. (2011).

Since November 2009 the GOME-2 AAI is an operational product in the O3M SAF. The GOME-2 level-1b data used for this paper were generated by PPF 4.0 and above. Reprocessed level-1b data are used from 5 January 2007 to 26 June 2008 (these are data from the so-called 'R01 reprocessing'), and for the period after this date the data were taken from the regular NRT flow of level-1b PDU data products that were disseminated by EUMETSAT via EUMETCast. The GOME-2 AAI level-2 product has a spatial resolution of 80 km by 40 km. Global coverage is achieved in 1.5 days, which makes the AAI also quite suitable for the detection and daily monitoring of forest fires and volcanic eruptions.

Verification of the retrieved degradation correction using the AAI

Using an offline GOME-2 AAI data processor we first calculate the residue (not taking any correction for instrument degradation into account) for the entire time range mentioned earlier. Then we calculate the daily global mean residue. The global mean residue is, in this case, defined as the mean residue of all measurements for a certain scan mirror position on a certain day between 60°N and 60°S with solar zenith angles less than 85 degrees. As reported in Tilstra et al. (2012), the global mean residue should normally be more or less constant in time, showing only a mild seasonal variation. In Figure 6 the calculated GOME-2 global mean residues are plotted as a function of time for each of the 24 scan mirror positions. The results are nearly identical to those presented earlier in Tilstra et al. (2010). The impact of instrument degradation is strong. At the end of the time series there is an east-west bias of almost 3 index points. Such an east-west bias complicates the use of the AAI product and without performing a correction the AAI would become useless.

Now we redo the entire analysis, with the one exception that this time we apply the correction for instrument degradation to the reflectances at 340 and 380 nm before we calculate the residues. The resulting global mean residues are plotted in Figure 6. Clearly, the effects of instrument degradation have been reduced strongly. We estimate that instrument degradation has been removed to within the 0.2 index point level. This number is somewhat larger than the number mentioned in Tilstra et al. (2012) for the SCIAMACHY instrument. The reason for this is that there are some jumps in the GOME-2 time series, related mainly to data processor version changes. These jumps are not removed

by the method. The jumps could potentially be handled by explicitly allowing jumps (discontinuities) at certain times t in the polynomial part P . However, we did not attempt to do this, firstly because the achieved improvement in Figure 6 is already satisfactory, and secondly, because most of the jumps will be gone as soon as the GOME-2 level-1b version 5.3 reprocessed data set is available and used.

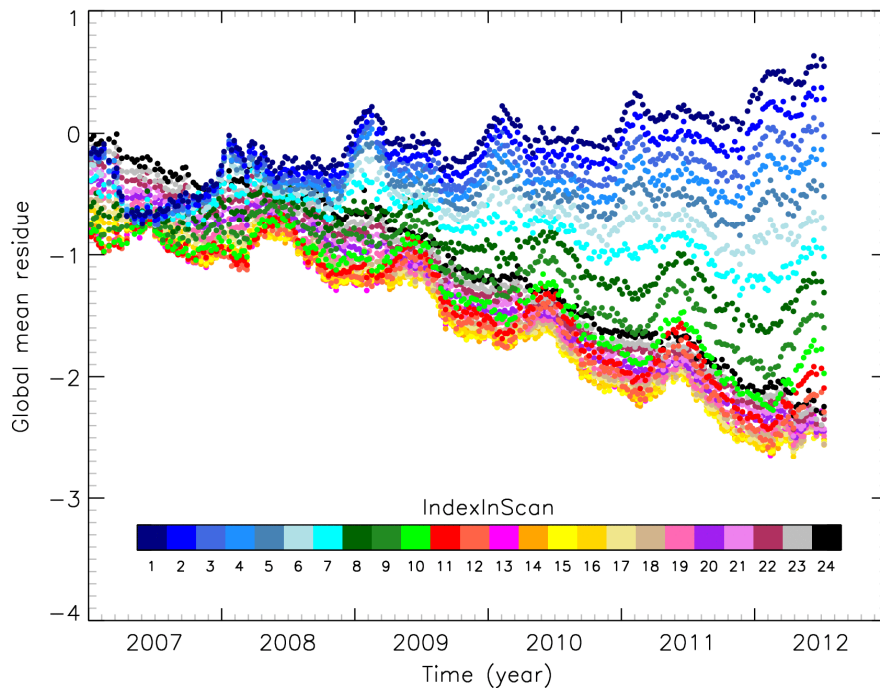


Figure 6: Time series of GOME-2 global mean residue, calculated for every seventh day using an offline AAI algorithm. Different colours relate to different scan mirror positions. There is very good agreement with results presented earlier in Tilstra et al. (2010). Notice the growing east-west bias. This is entirely caused by instrument degradation.

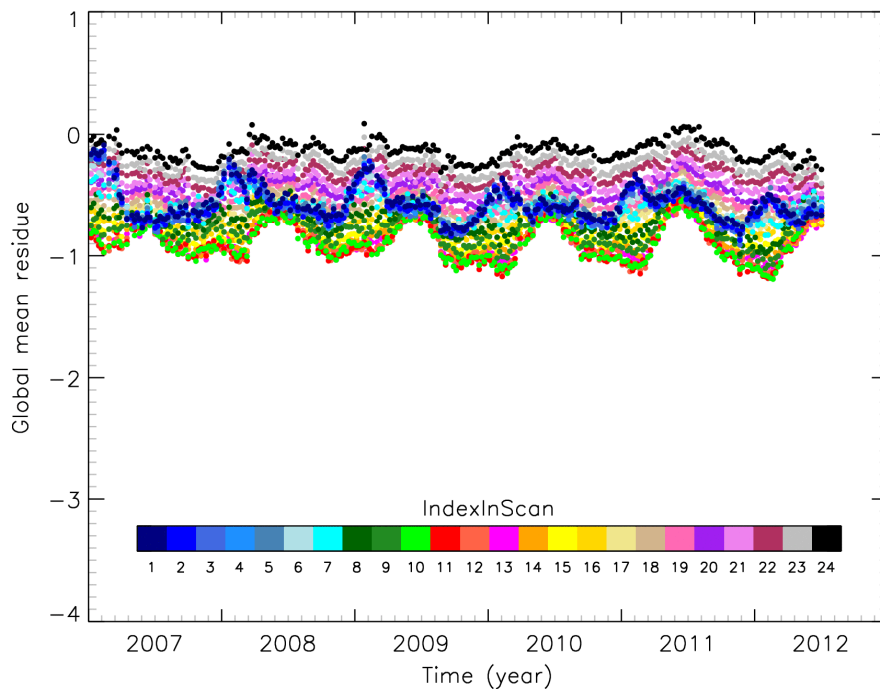


Figure 6: Same as the previous figure but now we applied our retrieved degradation correction parameters to the reflectances before calculating the residues. The effects of instrument degradation have disappeared almost completely.

SUMMARY

We showed that instrument degradation of the GOME-2 instrument on MetOp-A can be analysed well using the in-flight degradation correction method described in Tilstra et al. (2012). We analysed the degradation factor at several wavelength bands and conclude that instrument degradation does not only affect the shorter wavelengths, but also the longer wavelengths. The method also confirms that there is a large and growing east-west bias in the reflectance. This east-west bias had already been observed in level-2 products like the GOME-2 AAI. To verify the correctness of the retrieved correction factors, we apply these to the reflectances and calculate the GOME-2 AAI from those. Studying time series of global means of the AAI product, we find that instrument degradation is indeed strongly reduced. In conclusion, we have found that the GOME-2 Earth reflectance can be corrected well for the effects of instrument degradation using the proposed in-flight degradation correction method.

REFERENCES

Penning de Vries, M., Wagner, T., (2011) Modelled and measured effects of clouds on UV Aerosol Indices on a local, regional, and global scale. *Atmos. Chem. Phys.* **11**, 12715–12735, doi:10.5194/acp-11-12715-2011

Tilstra, L.G., Tuinder, O.N.E., Stammes, P., (2010) GOME-2 Absorbing Aerosol Index: Statistical analysis, comparison to GOME-1 and impact of instrument degradation. Proceedings of the 2010 EUMETSAT Meteorological Satellite Conference, EUMETSAT **P.57**, ISBN 978-92-9110-089-7

Tilstra, L.G., De Graaf, M., Aben, I., Stammes, P., (2012) In-flight degradation correction of SCIAMACHY UV reflectances and Absorbing Aerosol Index. *J. Geophys. Res.* **117**, D06209, doi:10.1029/2011JD016957